TA12 钛合金电子束焊接组织性能及残余应力分析

付鹏飞[1]， 黄 锐[2]， 刘方军[1]， 左从进[1]

（1. 北京航空制造工程研究所 高能束流加工技术国防科技重点实验室，北京 100024；
2. 成都飞机工业集团 钳焊导管厂，成都 610092）

付鹏飞

摘 要：采用电子束焊接 TA12 钛合金薄板焊缝表面成形良好，焊缝区以马氏体组织为主，细小的稀土相呈均匀弥散分布状态；随着距焊缝距离的增加，稀土相尺寸逐渐增大，数量逐渐减少，并逐渐趋于球形，沿接头呈一定的规律性分布。小孔法残余应力测试结果表明，垂直于焊缝方向残余应力以纵向应力主，应力呈梯度分布，横向应力较低；焊缝区为纵向拉应力区，应力峰值低于其屈服强度，横向应力为较小的压应力；沿焊缝试板中心区（±20 mm 范围内）焊接残余应力分布趋于稳定。

关键词：TA12 钛合金；电子束焊接；稀土相；残余应力

中图分类号：TG456.3 文献标识码：A 文章编号：0253－360X(2007)02－082－03

0 序 言

TA12 钛合金属近似于 α 型热强高温钛合金，是国内自行研制的可在 550 ℃下长期工作，又称作 Ti－55合金。该合金添加了稀土元素 Nd，在细化晶粒、净化晶界、稳定组织、提高抗氧化性等方面显示出良好的作用[1]。与国际上已采用的同类合金相比，TA12 钛合金在热稳定性与高温持久性能等方面都表现出较好的优势，可用于航空发动机压气机盘、鼓筒和叶片零件的制造。发动机零件的整体集成化加工需要对 TA12 钛合金材料进行焊接加工，由于电子束焊接具有诸多优点，因此，适合 TA12 钛合金的焊接及工程化应用需求。目前，国内对高温 TA12 钛合金焊接性能研究较少[2－4]，因此，针对 TA12 钛合金进行电子束焊缝组织性能及残余应力分析研究，对于其在航空发动机等领域的应用具有重要的意义。

1 材料及试验方法

TA12 钛合金试板厚度 1.5 mm，尺寸 300 mm×160 mm，其化学成分（质量分数，%）为 4.8～6.0 Al，0.75～1.25 Mo，3.7～4.7 Sn，1.5～2.5 Zr，0.6～1.2 Nd，0.20～0.35 Si，≤0.25 Fe 及微量杂质元素，其余为 Ti。在 ZD150－15B 电子束焊机上沿长度方向完成穿透焊缝，焊接工艺参数如表 1 所示。焊缝正面宽 1.6 mm，背面宽 0.7 mm，表面成形较好，焊缝正面形貌如图 1 所示。

表 1 TA12 钛合金电子束焊接工艺参数

Table 1 Parameter of EBW for TA12 titanium alloy

工艺	加速电压 U_a/kV	束流 I_b/mA	焊接速度 v/(mm·s^{-1})
焊接	120	4.1	10
修饰焊	120	2.1	5

图 1 TA12 钛合金电子束焊缝形貌

Fig. 1 TA12 alloy weld of EBW

2 试验结果及讨论

2.1 接头组织

TA12 钛合金电子束焊缝的组织形貌如图 2a 所示，由于在电子束的聚焦作用下，焊缝正面得到的热输入大于背面，其熔化的金属要比背面多，焊缝截面上宽下窄，呈现“倒三角”状，焊缝成形较好，未出现咬边现象，背面存在余高。

收稿日期：2006－03－28

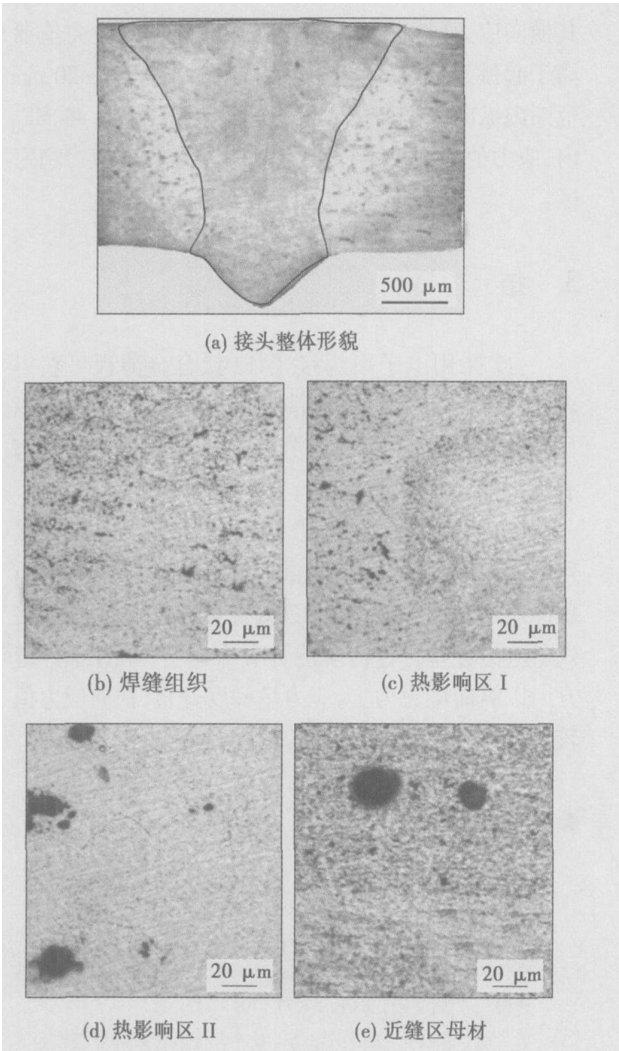

图 2　TA12 钛合金电子束焊接接头组织

Fig 2　Microstructure of EBW joint of TA12 titanium alloy

如图 2 所示，电子束焊缝熔合区存在大量细长的 α′马氏体及 α 相组织，分散细小的稀土相颗粒均匀分布于焊缝区；随着距焊缝距离的增加，过渡区马氏体组织逐渐减少，稀土相尺寸逐渐增大，数量逐渐减少；近缝区母材的稀土相尺寸更大并趋近球形，由针状 α 相加少量的 β 相组织组成。稀土相主要为 Nd 元素与 O，Sn 等元素形成的富钕稀土相，可阻碍位错的运动，细化晶粒，促进 ZrO_2 及 SiO_2 的选择性氧化析出和钉扎等作用，可提高合金抗高温和循环氧化性能[1]。各区域稀土相尺寸形态变化的原因是，在凝固过程中当温度降至合金基体的凝固点以下，稀土相形成元素在固液界面前沿的液相中富集，达到形核浓度时析出稀土相；在这一过程中存在着稀土相与凝固界面的交互作用，即存在一个临界速度，凝固速度高于这一临界值时，稀土相颗粒被捕获；低于这一临界值时，稀土相被推移并不断长大[5−7]。由于 TA12 钛合金电子束焊接速度较高，焊缝熔合区冷却速度极快，凝固界面的移动速度远高于临界值，稀土相颗粒来不及长大成形，即被移动的凝固界面捕获，获得无稀土相团聚的分布状态。所以焊缝区稀土相颗粒细小且均匀分布，远离焊缝尺寸增大数量减少。

2.2　焊接残余应力分布

根据前期的研究结果，选取小孔法对试板的焊接残余应力分布进行测试分析。考虑到平板焊接残余应力的分布特点，设计 *A*，*B*，*C* 三列及 *D* 行测点如图 3 所示，其中，*O* 点为中心，*B* 为中心线，*A*，*C* 与 *B* 间隔 20 mm，实际贴片照片如图 4 所示。

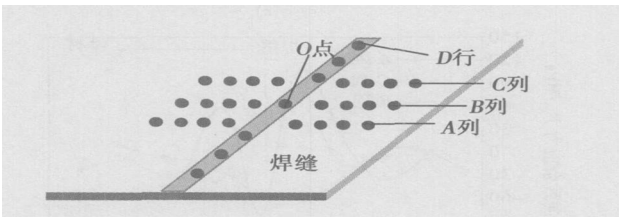

图 3　焊接试板测点布置

Fig 3　Schematic of measure location

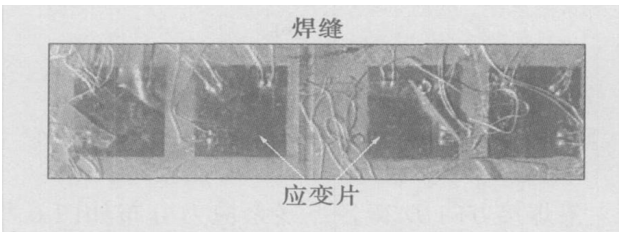

图 4　应变计贴片照片

Fig 4　Photograph of strain gauge pasted

采用的应变计阻值为 120 Ω±0.3 Ω，应变仪的灵敏系数为 2.07，钻孔直径为 2 mm。测试参照文献[8, 9]，每间隔 15 min 测试一次，同一测点总测试时间在 50 min 为宜。

通过小孔法测试的 TA12 钛合金平板垂直于焊缝各列残余应力分布如图 5 所示。*A*，*B*，*C* 三列的焊接残余应力梯度分布趋势基本相同，以焊缝为中心沿各列纵向应力梯度变化较大（400 ~200 MPa），焊缝区应力以纵向应力为主，横向应力值较小。焊缝区纵向拉应力峰值可达 404 MPa，远低于 TA12 钛合金材料的屈服强度及抗拉强度（文献[1]中抗拉强度为 980 MPa），沿各列远离焊缝纵向应力值逐渐减小，拉、压应力交替出现；焊缝区横向应力为压应力，沿各列方向拉压应力交替出现，应力值在±120 MPa 范围内变化；*A*，*C* 列焊缝及近缝区的纵向残余拉应力区宽 b_1 要小于 *B* 列的拉应力区宽 b_2，相应的拉

应力面积也小于中心线附近。

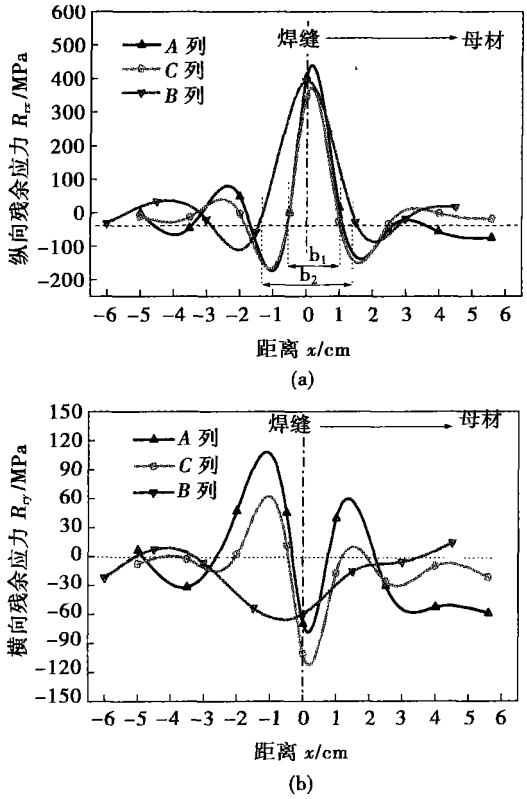

图 5 垂直于焊缝各列残余应力分布

Fig 5 Weld residual stresses along vertical direction

沿焊接方向 D 行各点残余应力分布如图 6 所示(包括 GAUSS FIT 高斯拟合曲线),焊缝区以纵向应力为主,应力值在 334 ~591MPa 内变化,远高于

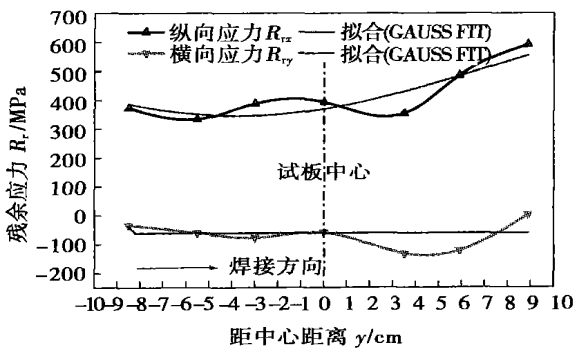

图 6 沿焊缝 D 行残余应力分布

Fig 6 Weld residual stresses along D in weld

其横向应力(-132 ~1.67 MPa);收弧部分应力值要高于起弧部分;以试板中心为原点,沿焊缝 ±20 mm 范围内纵向应力和横向应力梯度变化在 9 ~44 MPa 内,应力值趋于稳定,可近似将此区域看作应力稳定区。

3 结 论

(1) 采用电子束焊接 TA12 钛合金薄板可获得表面成形良好的焊缝,可消除咬边等缺陷,焊缝区以马氏体组织为主,组织成分均匀,稀土相尺寸、形态沿接头呈规律性分布。

(2) 采用小孔法测试 TA12 钛合金电子束焊接残余应力准确性较高,测试时间及过程可根据具体条件通过试验获得。TA12 钛合金薄板电子束焊接残余应力分布符合传统应力分布趋势,垂直于焊缝方向以纵向应力为主,应力呈梯度分布,横向应力值较低;焊缝区为纵向拉应力区,横向应力为压应力。

参考文献:

[1] 《中国航空材料手册》编辑委员会. 钛合金铜合金(第 4 卷)[M]. 北京:中国标准出版社, 2002.

[2] 郝传勇, 李正林, 毛先锋. Ti-55M 高温 Ti 合金焊缝塑性的改善[J]. 金属学报, 2001, 37(7): 709-712.

[3] 孟 鑫, 陈春焕, 姚向军, 等. Ti55 合金电子束焊缝氢致延迟裂纹的扩展机理[J]. 焊接学报, 2002, 23(4): 21-23.

[4] 郝传勇, 时元宝, 李正林, 等. Ti-5Al-4Sn-2Zr-1Mo-0.25Si-1Nd 合金焊接性[J]. 焊接学报, 2003, 24(3): 9-16.

[5] 李阁平, 王青江, 关少轩, 等. 快冷态与铸态 Ti-55 合金稀土相的研究[J]. 航空材料学报, 1994, 14(3): 19-26.

[6] 李阁平, 李 东, 刘羽寅, 等. 缓冷和快冷条件下 Ti-55 合金中稀土相的凝固特征[J]. 中国有色金属学报, 1999, 9(4): 683-687.

[7] 李阁平, 李 东, 刘羽寅, 等. 稀土相对 Ti-5.6Al-4.8Sn-2Zr-1Mo-0.32Si-1Nd 钛合金晶粒长大的阻碍作用[J]. 中国稀土学报, 2000, 18(4): 341-343.

[8] 唐慕饶. 焊接检测技术[M]. 北京:机械工业出版社, 1988.

[9] 游 敏, 郑小玲, 王福德. 盲孔法测定焊接残余应力适宜测试时间研究[J]. 武汉水利电力大学(宜昌)学报, 1999, 21(1): 54-57.

作者简介:付鹏飞,男,1978 年出生,助理工程师,硕士研究生。主要从事电子束焊接工艺及设备的研究工作,发表论文 5 篇。

Email: fupengfei97@163.com

Abstract: The electrical signals of CO_2 arc welding contain plenty of welding information. The joint time-frequency analysis was used to study the electrical signals of CO_2 arc welding. The effect of analysis window selecting of short-time Fourier transform to the result of time-frequency analysis spectrum was discussed, and the conclusion that Hanning window has better time-frequency centralizing in analysis was gotten. Based on several welding currents and arc voltages in experiment, the characteristic of energy distribution and metal transfer was investigated by time-frequency analysis to get the information of short-circuiting transfer in electrical signals of CO_2 arc welding. The result of analysis in experiment shows that more information in electrical signals can be gotten by time-frequency analysis in CO_2 arc welding. This way has a good foreground in research and application.

Key words: joint time-frequency analysis; CO_2 arc welding; short-time Fourier transform

Effect of thermit composition on manual SHS welding for low carbon steel LI Zhizun, XIN Wentong, WU Bin, LI Baofeng (Advanced Material Institute, Ordnance Engineering College, Shijiazhuang 050003, China). p79—81

Abstract: Base on self-propagating high-temperature synthesis(SHS), a new method of welding called manual SHS welding is introduced. Since it is easy to carry and operate, this technique can be used in emergency maintenance. The effect of the thermit composition of the combustion welding rod on the welding of low carbon steel and the microstructure of weld were studied. The thermit was composed of (CuO+Al) and (Fe_2O_3+Al). It is shown that when the content of (CuO+Al) is higher than 50%, welding can successfully proceed. And combustion velocity becomes higher with the increasing of (CuO+Al) content. This is due to the higher combustion temperature and larger combustion heat of (CuO+Al) thermit. The tensile strength of weld becomes higher with the increasing of (Fe_2O_3+Al) content. This is due to the precipitation of the second phase rich in Fe, which can thin the Cu grain and strengthen the alloy. The combustion welding rod with 50% and 60% (CuO+Al) thermit is easy to operate and the tensile strength of weld are higher than 420 MPa.

Key words: manual self-propagating high-temperature synthesis welding; thermit; combustion velocity; tensile strength

Microstructure and residual stress of TA12 titanium alloy with electron beam welding FU Pengfei[1], HUANG Rui[2], LIU Fangjun[1], ZUO Congjin[1](1. Key Laboratory of High Energy Density Beam Processing Technology, Beijing Aeronautical Manufacturing Technology Research Institute, Beijing 100024, China; 2. Qian Han Pipe Factory, Chengdu Aircraft Industrial Group Co., Ltd., Chengdu, 610092, China). p82—84

Abstract: Weld configuration of TA12 titanium alloy is very good for electron beam welding(EBW). The main microstructure of weld is martensite, and the tiny rare earth rich phases is dispersedly distributed in the weld zone, and dimension whose configuration changes disciplinary along the joint. By hole drilling method measuring weld residual stresses, the results show that longitudinal stresses are higher than transverse stress, which present gradient distribution along the vertical direction of the weld. In the weld all the longitudinal residual stresses are tensile stresses, and whose peak stresses are lower than yield stresses, while the transverse stresses are very low pressure stresses. Along the weld direction in the central of the plate the residual stresses distributing are approximate equal.

Key words: TA12 titanium alloy; electron beam welding; rare earth phase; residual stress

Effects of shielding gas in CO_2 laser—MAG hybrid welding GAO Ming, ZENG Xiaoyan, HU Qianwu, YAN Jun (School of Optoelectronics Science and Engineering, Huazhong University of Science and Technology, Wuhan 430074, China). p85—88

Abstract: Shielding gas is acrucial factor for the process stability, weld penetration and joint quality of CO_2 laser—MAG (mental active gas) hybrid welding. However, the concerned researches about this field are very few. A serial trial investigating the effect of He—Ar and CO_2—Ar shielding gas on CO_2 laser—MAG hybrid welding was carried out on mild steel. The results show that different mixed shielding gases have different effects. The penetration depth and microhardness of He—Ar welds are hisher than that of CO_2—Ar welds. Because atomic oxygen is decomposed from CO_2 under high temperature and enters into welding pool, the surface tension coefficient changes and the direction of weld pool flow is changed. Consequently, CO_2—Ar weld reinforcement becomes flatter at $CO_2 \geqslant 30\%$ and the transition from arc zone to laser zone is flatter. Moreover, when $CO_2 > 30\%$, the process stability and microhardness of weld dramatically decrease.

Key words: laser welding; arc welding; hybrid welding; shielding gas; welding penetration

A CO_2 arc welding seam detection algorithm based on transition region YANG Fugang, SUN Tongjing, ZHANG Guangxian, PANG Qingle (School of Control Science and Engineering, Shandong University, Jinan 250061, China). p89—91

Abstract: In order to detect CO_2 arc welding seam, a new image segmentation method based on transition region is presented. Transition region is a special region located between the object and background in the real image, whose histogram has a wide and evenly hollow between two peaks. First, transition region of original image is determined by calculating the average grads of nonzero pixels of the image obtained through top-cut and bottom-cut transform, and then threshold can be obtained easily from transition region. It overcomes the effect of disturbance. Examinations indicate that it is a good method to detect CO_2 arc welding seam.

Key words: CO_2 arc welding; edge detection; seam detection; transition region

Application of vibratory welding technology to large-scale welding components LU Qinghua, CHEN Ligong, NI Chunzhen, RAO Delin (School of Materials Science and Engineering, Shanghai Jiaotong University, Shanghai 200030, China). p92—94, 98

Abstrat: The vibratory conditioning process was investigated